The EMBO Journal Vol. 20 No. 8 pp. 1863–1874, 2001

Perinuclear, perigranular and sub-plasmalemmal mitochondria have distinct functions in the regulation of cellular calcium transport

Myoung Kyu Park[1,2], Michael C.Ashby[1], Gul Erdemli[1], Ole H.Petersen[1,3] and Alexei V.Tepikin[1]

[1]MRC Secretory Control Research Group, The Physiological Laboratory, University of Liverpool, UK

[2]Present address: Department of Physiology, Sungkyunkwan University School of Medicine, Suwon 440-746, Korea

[3]Corresponding author
e-mail: o.h.petersen@liv.ac.uk

We have identified three distinct groups of mitochondria in normal living pancreatic acinar cells, located (i) in the peripheral basolateral region close to the plasma membrane, (ii) around the nucleus and (iii) in the periphery of the granular region separating the granules from the basolateral area. Three-dimensional reconstruction of confocal slices showed that the perigranular mitochondria form a barrier surrounding the whole of the granular region. Cytosolic Ca^{2+} oscillations initiated in the granular area triggered mitochondrial Ca^{2+} uptake mainly in the perigranular area. The most intensive uptake occurred in the mitochondria close to the apical plasma membrane. Store-operated Ca^{2+} influx through the basolateral membrane caused preferential Ca^{2+} uptake into sub-plasmalemmal mitochondria. The perinuclear mitochondria were activated specifically by local uncaging of Ca^{2+} in the nucleus. These mitochondria could isolate nuclear and cytosolic Ca^{2+} signalling. Photobleaching experiments indicated that different groups of mitochondria were not luminally connected. The three mitochondrial groups are activated independently by specific spatiotemporal patterns of cytosolic Ca^{2+} signals and can therefore participate in the local regulation of Ca^{2+} homeostasis and energy supply.

Keywords: Ca^{2+} transport/mitochondria/perigranular/perinuclear/sub-plasmalemmal

Introduction

Much recent Ca^{2+} signalling work has dealt with the importance of the mitochondria. Contrary to conclusions from earlier work, it is now clear that mitochondria can and do take up Ca^{2+} during normal Ca^{2+} signalling events and then release it much more slowly (Pozzan *et al*., 1994, 2000; Duchen, 2000; Rutter and Rizzuto, 2000). Ca^{2+} in the mitochondria is of importance for the regulation of metabolism, since three dehydrogenases of the Krebs cycle are modulated by the Ca^{2+} concentration in the micromolar range (Denton and McCormack, 1990; McCormack *et al*., 1990). Repetitive cytosolic Ca^{2+} spikes induce mitochondrial Ca^{2+} spikes. Each spike is sufficient to cause a maximal transient activation of the Ca^{2+}-sensitive mitochondrial dehydrogenases and above a certain frequency there is sustained activation of mitochondrial metabolism (Hajnoczky *et al*., 1995). Agonist stimulation, evoking cytosolic and mitochondrial Ca^{2+} signals, elicits increases in both the mitochondrial and cytosolic ATP concentrations that depend on both the amplitude of the Ca^{2+} rise inside the mitochondria and the availability of mitochondrial substrates. Thus, mitochondrial Ca^{2+} plays a direct role in driving ATP production (Jouaville *et al*., 1999). Mitochondrial Ca^{2+} uptake is also important for the regulation of other processes. In chromaffin cells, stimulation triggers fast millimolar mitochondrial Ca^{2+} transients and these can modulate secretion (Montero *et al*., 2000). In pancreatic acinar cells, active mitochondria localized in a belt surrounding the granular region are important for confining cytosolic Ca^{2+} signals initiated in this region to this part of the cell, where secretion is regulated (Tinel *et al*., 1999; Straub *et al*., 2000). It has been shown recently that respiring mitochondria determine the pattern of activation and inactivation of the store-operated Ca^{2+} inflow that is of importance for refilling endoplasmic reticulum (ER) stores with Ca^{2+} lost during agonist stimulation (Gilabert and Parekh, 2000).

It has been proposed that the localization of mitochondria with respect to Ca^{2+} sources can be a determinant of their Ca^{2+} uptake kinetics (Lawrie *et al*., 1996). It would be desirable to test this critically in intact polarized cells, where different groups of mitochondria could be clearly identified in relation to other subcellular structures and in particular in relation to specific subcellular Ca^{2+} release sites. Here we have investigated, in normal polarized pancreatic acinar cells, how mitochondria positioned in specific subcellular locations respond to various patterns of cytosolic Ca^{2+} ($[Ca^{2+}]_i$) signals. We identified three distinct groups of mitochondria located (i) in the peripheral basolateral region very close to the plasma membrane, (i) around the nucleus and (iii) in the periphery of the granular region separating the apical granular area from the basolateral part of the cell. When $[Ca^{2+}]_i$ was increased uniformly throughout the cell, by global uncaging of caged Ca^{2+}, we found no regional differences in mitochondrial Ca^{2+} uptake. In experiments where we used UV laser-induced local bleaching of an intra-mitochondrial dye, we saw no evidence of luminal connectivity between mitochondria in different regions. $[Ca^{2+}]_i$ oscillations initiated in the granular area triggered mitochondrial Ca^{2+} uptake mainly in the perigranular area. Ca^{2+} influx through the basolateral membrane, generated by emptying intracellular Ca^{2+} stores, elicited Ca^{2+} uptake into nearby peripheral basolateral mitochondria. Perinuclear mitochondria were specifically activated by local Ca^{2+} release in the nucleus. Distinct groups of separate mitochondria,

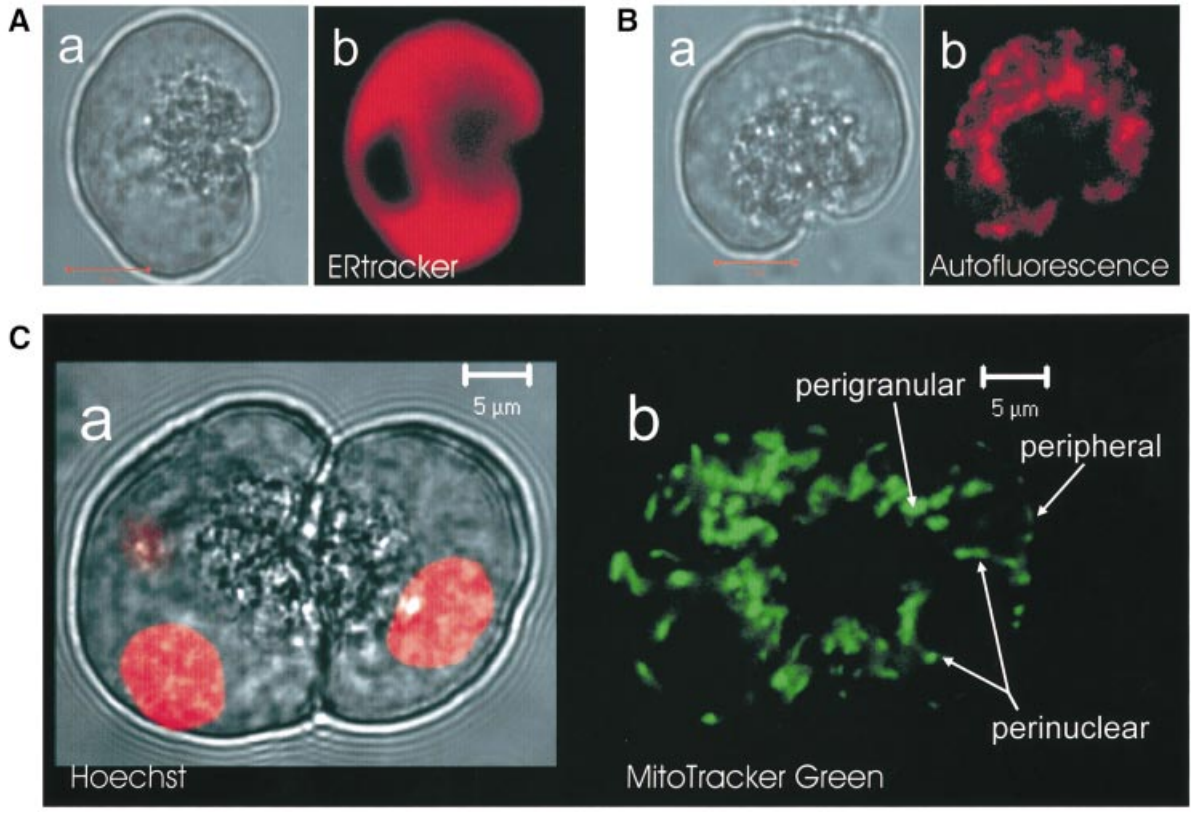

Fig. 1. Localization of endoplasmic reticulum (ER), nuclei and mitochondria in living pancreatic acinar cells. (**A**) Endoplasmic reticulum. The transmitted light picture of a single isolated acinar cell is shown in (a). In (b), the fluorescence image obtained with ERtracker is shown. The ER is densely packed outside the granular and nuclear areas. (**B**) Mitochondria. Transmitted light picture in (a) and autofluorescence (NADH) image in (b). The mitochondria are localized principally as a belt surrounding the granular region and as a peripheral ring just under the plasma membrane. Lengths of red bars in (A, a) and (B, a) represent 10 μm. (**C**) Nuclei and mitochondria. (a) Transmitted light picture showing the typical structure of two connected acinar cells with the secretory (zymogen) granules in the central part surrounding what in the intact organ would be the lumen. The nuclei are stained red with Hoechst 33342 and the fluorescence image is superimposed on the transmitted light picture. In the cell on the left, the focal plane goes through one nucleus, but it is just possible to detect the presence of a second nucleus. (b) MitoTracker Green fluorescence image. The strongest staining is localized as a ring surrounding the granular area, with some staining at the periphery as well as around the three nuclei (two in the left and one in the right cell). The mitochondria surrounding the nuclei seem to be aligned along the surfaces of these organelles.

due to their strategic positioning within the cell, can therefore sense and shape $[Ca^{2+}]_i$ signals locally to help the cell regulate activities in specific subcellular compartments and ensure adequate local energy supply.

Results

The relative positions of granules, mitochondria, ER and nucleus in the living pancreatic acinar cells

The polarization of pancreatic acinar cells with the ER and the nucleus in the basolateral part and the granules in the apical pole was well maintained even after isolation of single cells, as shown in Figure 1. There was heavy staining with ERtracker in the basolateral areas surrounding the granular region, except in the nucleus (n = 6) (Figure 1A). The granules were localized in the apical pole close to the tiny apical (luminal) membrane. High resolution confocal images of NADH autofluorescence showed the locations of the mitochondria, which were predominantly grouped in a central perigranular area and in a peripheral area close to the plasma membrane (n = 26) (Figure 1B). This is similar to what we have shown previously with the help of MitoTracker Green (Tinel *et al*., 1999) and tetramethyl rhodamine ethyl ester (Raraty *et al*., 2000) fluorescence. In some experiments we used both MitoTracker Green FM, to check the mitochondrial distribution, and Hoechst 33342, to visualize the nuclei, simultaneously. In these cells we saw that there was also a group of mitochondria close to and sometimes surrounding the nucleus (Figure 1C) (n = 10).

Mitochondrial Ca^{2+} uptake following acetylcholine (ACh)-elicited release of Ca^{2+} from the endoplasmic reticulum

To image mitochondria and measure the mitochondrial Ca^{2+} concentration ($[Ca^{2+}]_m$), we used the Ca^{2+}-sensitive dye Rhod-2, which is concentrated in compartments with a highly negative voltage (Pinton *et al*., 2001). The transmitted light picture of a cell under investigation is shown in Figure 2A. The mitochondrial distribution is disclosed in Figure 2B. After exposing the cell to Rhod-2-AM, the fluorescence intensity was generally weak, in the absence of stimulation, as shown in Figure 2C1. However, after ACh (10 μM) application the characteristic localization of mitochondria was revealed gradually and finally the Rhod-2 fluorescence image (Figure 2C6) was similar to the picture obtained imaging the NADH autofluorescence (Figure 2B). This suggests that the initial low Rhod-2

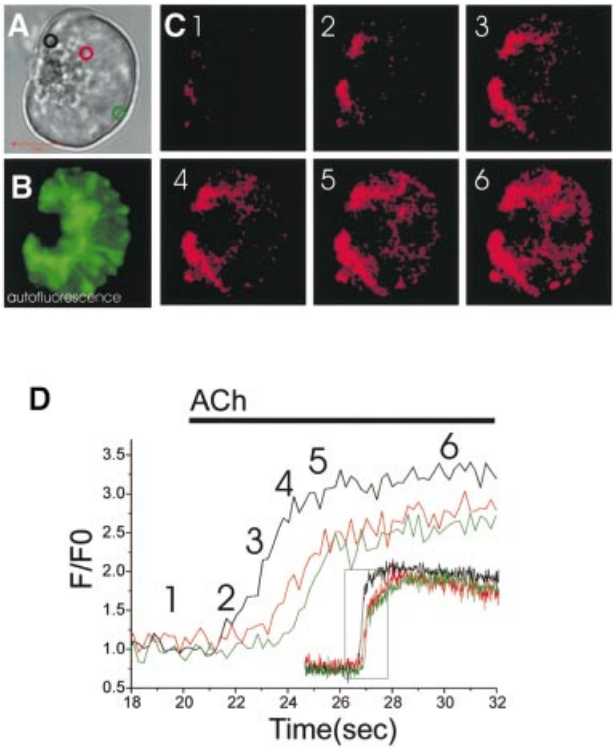

Fig. 2. Mitochondrial Ca^{2+} uptake, measured with Rhod-2, following maximal ACh (10 μM)-elicited Ca^{2+} release from the endoplasmic reticulum. (**A**) Transmitted light picture showing the cell under investigation, with the three areas of interest identified by the three coloured circles. The length of the red bar represents 10 μm. (**B**) Autofluorescence image showing mitochondrial localization. (**C**) Six images showing mitochondrial Ca^{2+} concentration. Image 1 shows the situation just before the start of stimulation. Image 2 shows that immediately after ACh application, there was Ca^{2+} uptake into mitochondria very close to the apical membrane. A little later, the whole perigranular mitochondrial belt was revealed (images 3 and 4) and finally (images 5 and 6) all mitochondria in the cell had taken up Ca^{2+}. (**D**) The time course of the mitochondrial Ca^{2+} uptake in the three regions identified in (A) using the appropriate colour coding. The main part of the figure represents a short time segment of the more complete traces shown in the inset. The time scale relates to the expanded traces labeled with the numbers 1–6, corresponding to the images in (C).

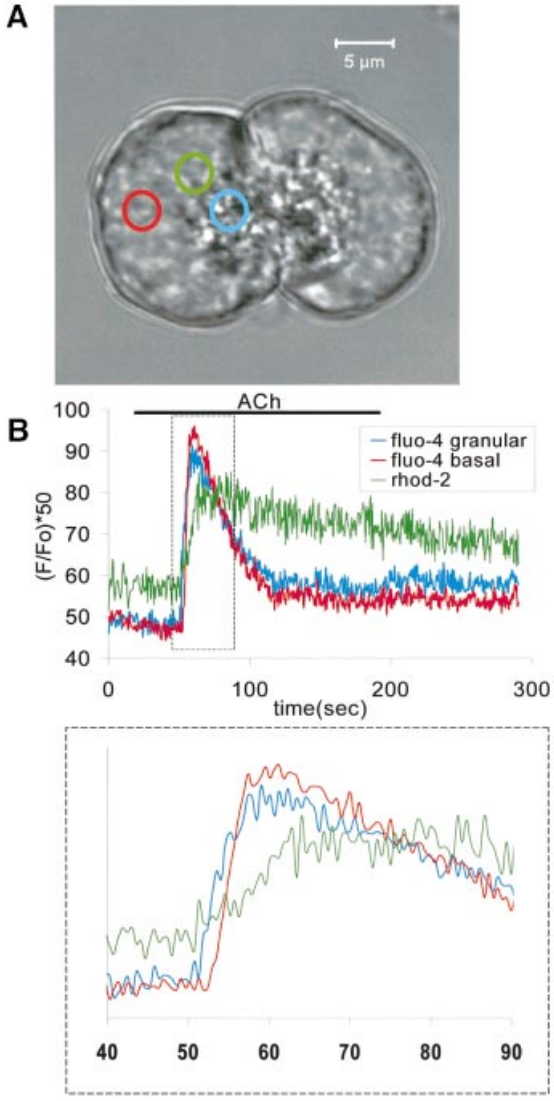

Fig. 3. Simultaneous measurements of cytosolic (fluo-4) and mitochondrial (Rhod-2) Ca^{2+} concentration changes after ACh stimulation. (**A**) The transmitted light picture shows the structure of the acinar doublet with the three colour-coded circles indicating the regions of interest. (**B**) The time courses of the ACh-elicited changes in the cytosolic Ca^{2+} concentrations in the granular (blue) and basal (red) regions, as well as the mitochondrial Ca^{2+} concentration in the perigranular region (green). In the inset below, showing the initial part of the three curves on an expanded time scale, it is seen that the mitochondrial Ca^{2+} uptake started immediately after the initial rise in the cytosolic Ca^{2+} concentration in the granular area.

fluorescence intensity was due to the relatively low resting $[Ca^{2+}]_m$ and not caused by insufficient mitochondrial dye loading. Mitochondrial Ca^{2+} uptake occurred, at first, in the lateral area close to the apical membrane and thereafter spread to the basolateral part of the cell (Figure 2C and D). Mitochondrial Ca^{2+} uptake was rapid and the maximal $[Ca^{2+}]_m$ was reached within ~5 s as seen in Figure 2D, which shows the changes of fluorescence intensity measured in three differently located mitochondria marked in Figure 2A (black, red and green circles). The average time lag between the mitochondrial Ca^{2+} rise in the lateral area close to the apical membrane (black trace) and at the base of the cell (green trace) was 2.4 ± 0.2 s (n = 7).

In general, the mitochondrial Ca^{2+} uptake in response to an ER-derived rise in the cytosolic Ca^{2+} concentration has been shown to occur immediately (Rizzuto *et al*., 2000). However, in a recent study on pancreatic acinar cells, it has been reported that there is a substantial delay of ~10 s, after the initiation of the cytosolic Ca^{2+} signal, before a measurable rise in the mitochondrial Ca^{2+} concentration is seen (Gonzalez *et al*., 2000). In view of these surprising results, we carried out experiments in which changes in the Ca^{2+} concentration in the cytosol and the mitochondria were monitored simultaneously, by measurement of fluo-4 and Rhod-2 fluorescence, in order to evaluate how quickly the mitochondrial Ca^{2+} uptake mechanism responded to the cytosolic Ca^{2+} signal. We saw no evidence of a substantial delay between the initiation of the cytosolic and mitochondrial Ca^{2+} signals. Figure 3 shows the result from one of these experiments. ACh elicited a cytosolic Ca^{2+} wave, which was initiated in the granular pole and then moved towards the base and reached the basal region within ~2 s. As seen in Figure 3, the initial rise in $[Ca^{2+}]_m$ coincided with the initial rise in $[Ca^{2+}]_i$, although the peak

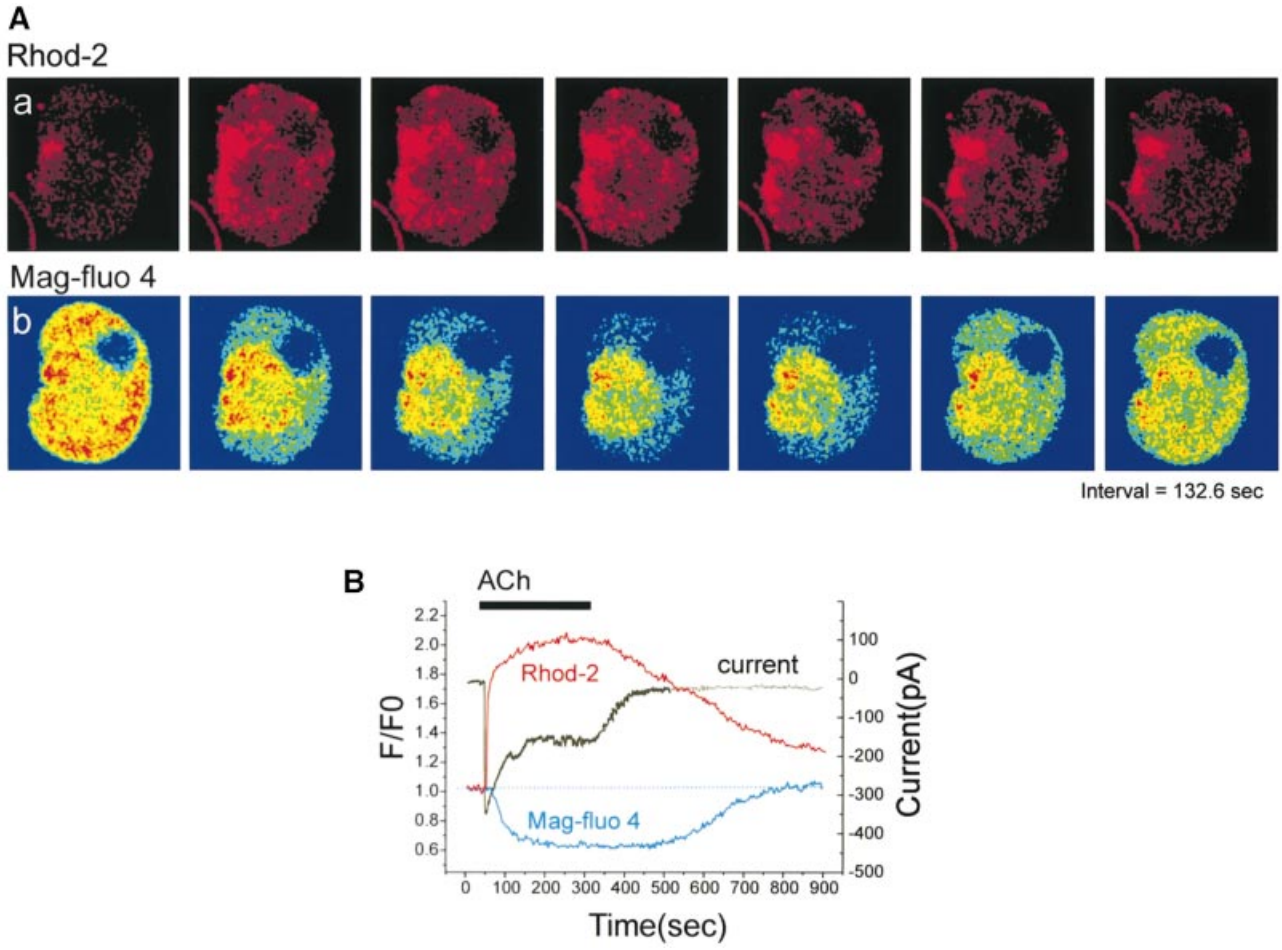

Fig. 4. Simultaneous measurements of the ACh-elicted Ca^{2+} concentration changes in the ER and the mitochondria. (**A**) Images from a single cell. (a) Rhod-2 fluorescence images taken at 132.6 s intervals showing the accumulation and subsequent loss of Ca^{2+} from the mitochondria following a short period of ACh stimulation. The first image was obtained just before the start of stimulation with ACh. (b) Mag-fluo-4 fluorescence images showing the gradual loss of Ca^{2+} from the ER in response to ACh stimulation and the subsequent re-accumulation. The first image was taken just before the start of stimulation. The interval between images was 132.6 s. (**B**) Time course of ACh-elicited changes in the Ca^{2+} concentrations in the mitochondria (Rhod-2, red), the ER (Mag-fluo-4, blue) and the cytosol (whole-cell Ca^{2+}-dependent current, black).

$[Ca^{2+}]_m$ was attained later than the peak $[Ca^{2+}]_i$. Six experiments of this type gave similar results.

The ER is the main Ca^{2+} storage organelle as well as a main supplier of Ca^{2+} to the mitochondria. Therefore, we measured $[Ca^{2+}]_m$, the Ca^{2+} concentration in the ER ($[Ca^{2+}]_{ER}$) and $[Ca^{2+}]_i$ simultaneously in the same cell. To do this, we exposed cells to Rhod-2-AM and the low affinity Ca^{2+}-sensitive dye Mag-fluo-4-AM (K_d = 22 μM). Thereafter, we introduced a patch pipette (whole-cell recording configuration) to wash out the cytosolic dye components. The time course of changes in $[Ca^{2+}]_i$ was assessed by measurement of the Ca^{2+}-dependent current (Petersen, 1992). Since the ER is mainly located in the basolateral part of the cell (Figure 1A), the decrease in $[Ca^{2+}]_{ER}$ was observed mainly in the basolateral region (Figure 4), as demonstrated previously (Park *et al*., 2000). As discussed extensively (Park *et al*., 2000; Petersen *et al*., 2001), this is entirely consistent with the well established finding that the $[Ca^{2+}]_i$ rise is initiated in, and often confined to, the apical granular pole. The Ca^{2+} release occurs from very tiny extensions of the basolateral ER into the apical pole, which is dominated by granules. The $[Ca^{2+}]_m$ change was mainly in the perigranular (particularly marked in the lateral area close to the apical membrane) and peripheral areas (Figure 4A, a). The Mag-fluo-4 fluorescence intensity in the perigranular (mitochondrial) area was initially slightly increased after application of ACh, which could be due to some of the dye being trapped in the mitochondria. This phenomenon was abolished by application of mitochondrial metabolic blockers (1 μM oligomycin and 1 μM rotenone; n = 6) or dialysis of a 10 mM BAPTA/2 mM Ca^{2+} mixture through the patch pipette (n = 17). We plotted the time course of the ACh-elicited changes in $[Ca^{2+}]_i$ (Ca^{2+}-dependent Cl^- current), $[Ca^{2+}]_m$ (Rhod-2 fluorescence) and $[Ca^{2+}]_{ER}$ (Mag-fluo-4 fluorescence) together in Figure 4B. After ACh stimulation, $[Ca^{2+}]_i$ and $[Ca^{2+}]_m$ increased immediately, even before there was a measurable decrease in $[Ca^{2+}]_{ER}$. After washout of ACh, $[Ca^{2+}]_i$ returned much more quickly to the resting level than $[Ca^{2+}]_{ER}$ and $[Ca^{2+}]_m$. The mitochondria released Ca^{2+} and the ER refilled with Ca^{2+} without provoking any Ca^{2+}-dependent current, indicating the possibility of Ca^{2+} recycling between mitochondria and nearby ER elements. The mitochondrial Ca^{2+} release following the Ca^{2+} uptake was very slow (see Figure 4). This phenomenon was

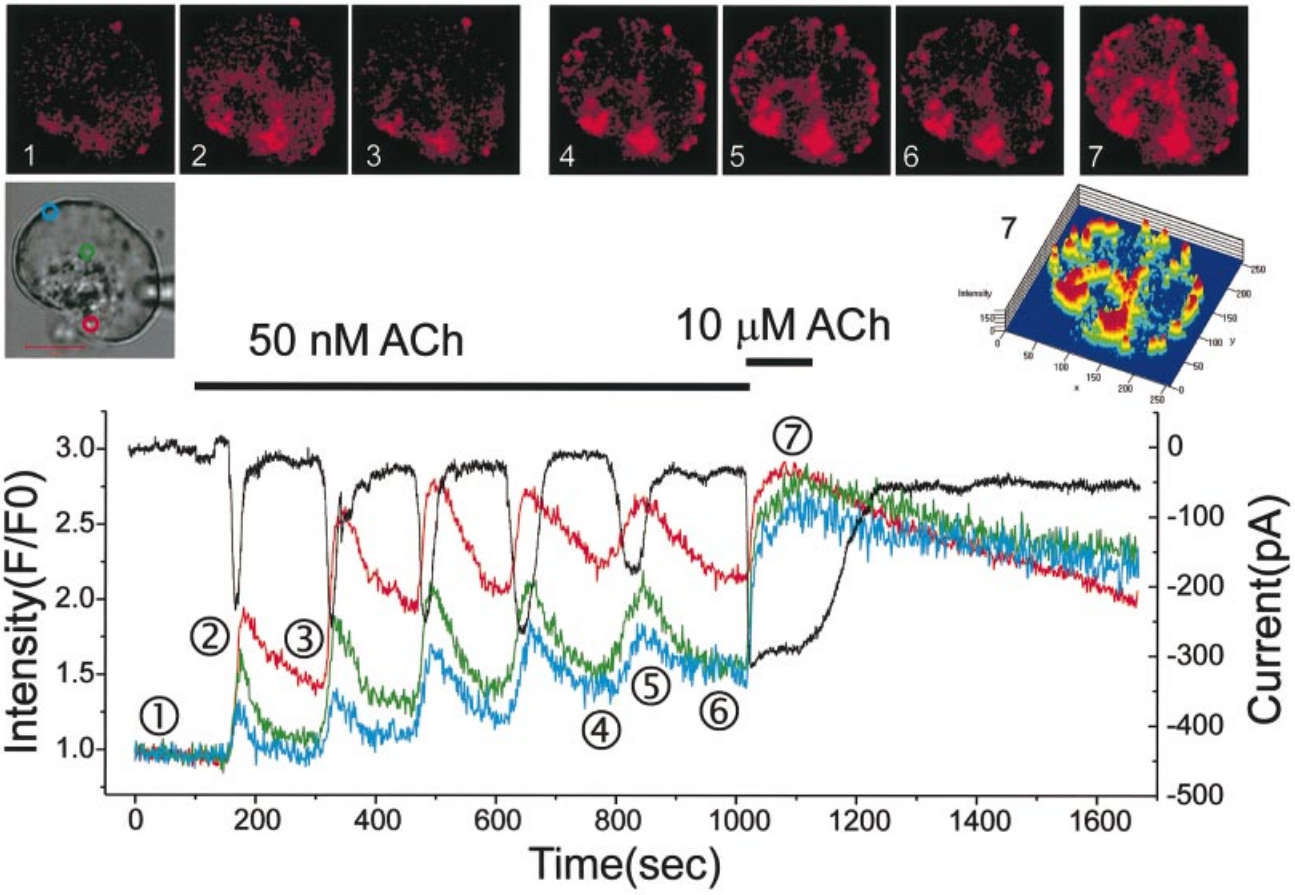

Fig. 5. Region-specific mitochondrial Ca^{2+} uptake following cytosolic Ca^{2+} oscillations. The coloured traces in the main panel show the time courses of the Ca^{2+} concentration changes in mitochondria localized as shown in the transmitted light image. The colour coding of the traces corresponds to the coloured circles in the transmitted light picture. The length of the red bar in the transmitted light picture corresponds to 10 μm. The black trace in the main panel represents the Ca^{2+}-dependent whole-cell current, which shows the time course of the changes in the cytosolic Ca^{2+} concentration. Stimulation with a low ACh concentration elicited repetitive cytosolic Ca^{2+} spikes. The Rhod-2 fluorescence images taken before, during and after the first ACh-elicited cytosolic Ca^{2+} spike (images 1–3) show that the main mitochondrial Ca^{2+} uptake during this spike occurred in the perigranular region. Since the release of Ca^{2+} taken up into the mitochondria is relatively slow, the mitochondria did not liberate all the Ca^{2+} accumulated during a single spike before the next spike occurred. Therefore, during this experiment, Ca^{2+} accumulated gradually in the mitochondria. In relation to the last spike in the series, the corresponding Rhod-2 fluorescence images are shown (images 4–6). It can be seen that even before the spike started there was considerable fluorescence both from the most apically located mitochondria in the perigranular ring and also from the peripheral ring close to the plasma membrane. During the spike there was increased fluorescence in all mitochondrial regions, which then declined after the spike. Finally, the cell was stimulated maximally by a high ACh concentration, causing a marked increase in the cytosolic Ca^{2+} concentration, as seen in the electrophysiological trace and futher mitochondrial Ca^{2+} accumulation (image 7).

similar in intact Rhod-2-loaded cells (n = 12) and cells dialysed via a patch pipette (n = 6). The time course was somewhat variable from cell to cell, but usually it took >10 min to restore $[Ca^{2+}]_m$ to the pre-stimulation level after a period of supramaximal ACh (10 μM) stimulation. The mitochondrial Ca^{2+} uptake was particularly marked in the lateral area close to the apical membrane (Figure 4A, a), which is very close to the primary ER Ca^{2+} release site (trigger zone) (Kasai *et al*., 1993; Mogami *et al*., 1997; Cancela *et al*., 2000). Also, after washout of ACh, the Ca^{2+} extrusion was particularly slow in these mitochondria.

In the pancreatic acinar cell, it is well known that low doses of ACh or cholecystokinin (CCK) generate $[Ca^{2+}]_i$ oscillations, which always start close to the apical membrane and are mostly confined to the granular area (Thorn *et al*., 1993). It has been suggested that the perigranular mitochondria provide a Ca^{2+} buffer barrier, which prevents or reduces the degree of Ca^{2+} signal spreading to the basolateral region (Tinel *et al*., 1999). However, so far there has been no direct demonstration of Ca^{2+} uptake into the perigranular mitochondria during Ca^{2+} spiking. We therefore evoked $[Ca^{2+}]_i$ oscillations with a relatively low dose of ACh and observed $[Ca^{2+}]_m$ changes in different parts of the cell. To monitor the $[Ca^{2+}]_i$ oscillations we measured the Ca^{2+}-dependent current. In the experiment illustrated in Figure 5, ACh (50 nM) elicited repetitive $[Ca^{2+}]_i$ spikes. The individual spikes were initially short-lasting and largely confined to the apical granular area (i.e. large cytosolic Ca^{2+} concentration gradient between apical and basolateral regions during the spike), but gradually became broader and global. The initial cytosolic Ca^{2+} spike was associated with a marked Ca^{2+} uptake into the perigranular mitochondria. In the Rhod-2 fluorescence images shown in Figure 5, the mitochondrial perigranular belt was invisible before the first ACh-elicited Ca^{2+} spike (image 1), but at the height of the spike the perigranular mitochondrial belt was clearly delineated (image 2). After the spike, the image of the

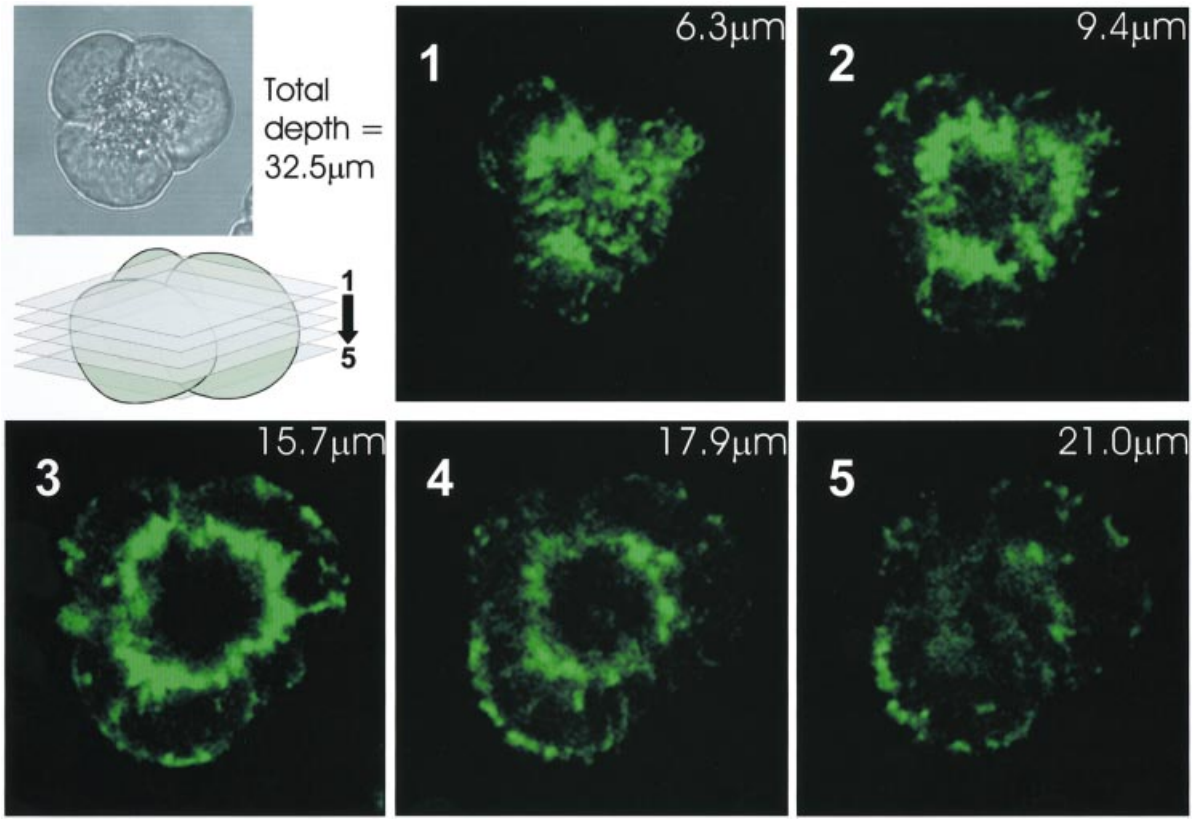

Fig. 6. Serial confocal sectioning reveals essentially complete perigranular mitochondrial belt. An acinar cell triplet (inset transmitted light image) was loaded with Rhod-2 and stimulated maximally with ACh. After the peak response, several confocal sections (see schematic illustration) revealed the almost complete coverage of the granular region by mitochondria. The thickness of the confocal sections was 3.5 μm.

perigranular belt disappeared (image 3). At the height of the first spike there was little sign of Ca^{2+} uptake into the mitochondria in other parts of the cell. Later, when the cytosolic Ca^{2+} spikes became broader and global, Ca^{2+} accumulated both in the perigranular belt and in the peripheral sub-plasmalemmal region (image 4). This was due to the relatively slow Ca^{2+} liberation from the mitochondria. During each spike, Ca^{2+} was taken up and then subsequently released, but the release was so slow that when the next spike occurred, all Ca^{2+} taken up during the previous spike had not yet been liberated. In this phase, the cytosolic Ca^{2+} spike was associated with mitochondrial Ca^{2+} uptake both in the perigranular belt and in the peripheral region (image 5). There was a visible, but minor, reduction in the mitochondrial Ca^{2+} concentration following the spike (image 6). Finally, a high concentration of ACh elicited a marked increase in the fluorescence intensity in the perigranular belt, the peripheral region and near the nucleus (image 7). Five experiments of this type all gave similar results.

In view of the functional importance of the perigranular mitochondrial belt, we investigated to what extent these mitochondria form a complete barrier around the granules. Using serial confocal slicing through Rhod-2-stained cells, after a maximal ACh-elicited Ca^{2+} signal had caused substantial Ca^{2+} uptake into the mitochondria, it was possible to see that the mitochondria essentially cover the whole surface of the granular area, like the skin on a football (Figure 6).

Mitochondrial Ca^{2+} uptake in response to uncaging of caged Ca^{2+} in the cytosol and the nucleus

In order to investigate the time course of mitochondrial Ca^{2+} uptake in different regions, we tried to abruptly increase $[Ca^{2+}]_i$ globally or locally by uncaging of Ca^{2+} from the caged Ca^{2+} compound *o*-nitrophenyl (NP)-EGTA. To prevent Ca^{2+} induction of Ca^{2+} release from the ER, we incubated the cells in Ca^{2+}-free solution containing 1 μM thapsigargin for 10 min. Thereafter, we introduced a patch pipette (whole-cell configuration) containing 1.2–1.5 mM NP-EGTA. Figure 7 shows an example of such an experiment (n = 5). The transmitted light picture of the cell with the three regions of interest identified by circles in different colours and the outline of the experimental arrangement is shown in Figure 7A, a and b. When Ca^{2+} was uncaged throughout all regions of the cell, to produce a uniform global rise in $[Ca^{2+}]_i$, we observed that mitochondrial Ca^{2+} uptake occurred simultaneously everywhere and reached a peak after ~4 s (Figure 7A, c). $[Ca^{2+}]_i$ was monitored by measurement of the Ca^{2+}-sensitive whole-cell current. The initial part of Figure 7A, c is expanded in Figure 7A, d, where it can be seen more clearly that there was no detectable difference in the kinetics of the mitochondrial Ca^{2+} uptake in the different parts of the cell. The regions of interest are marked in Figure 7A, a with colours corresponding to the traces in Figure 7A, c and d. These experiments demonstrate the high rate of mitochondrial Ca^{2+} uptake and the absence of a significant delay to the start of Ca^{2+}

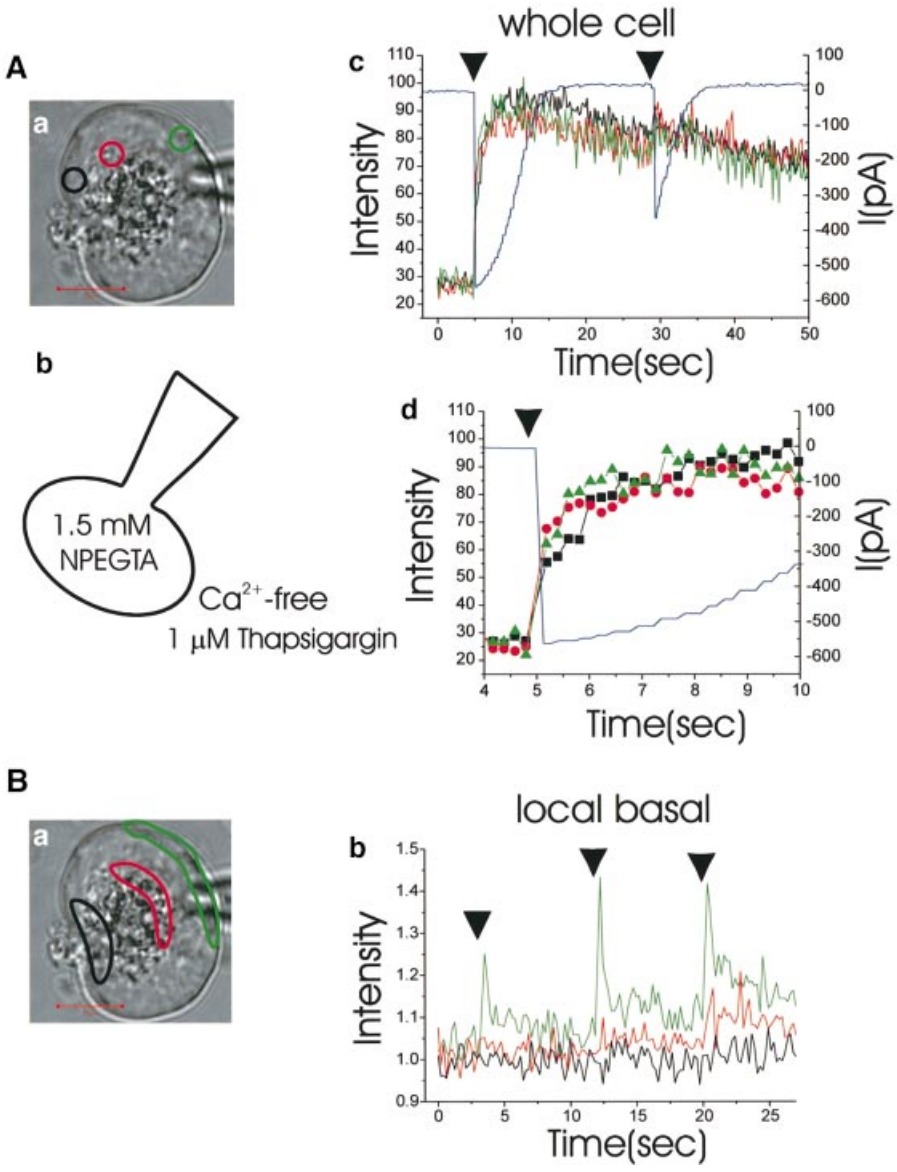

Fig. 7. Local and global uncaging of caged Ca^{2+} causes local and global mitochondrial Ca^{2+} uptake. (**A**) Global uncaging. (a) Transmitted light picture showing the three colour-coded regions of interest. Length of red bar corresponds to 10 μm. (b) Schematic diagram indicating recording configuration and experimental arrangement. (c) Time course of mitochondrial Ca^{2+} uptake, in the three colour-coded regions identified in (A, a), following two separate global cytosolic Ca^{2+} uncagings (arrowheads). The uncagings cause large increases in the cytosolic Ca^{2+} concentration (monitored as Ca^{2+}-dependent current). It is seen that this is associated with a uniform increase in the Rhod-2 fluorescence in all regions. (d) An expanded time scale showing the first part of the response to the first uncaging of Ca^{2+}. (**B**) The effect of local Ca^{2+} uncaging in the basal region. (a) Transmitted light picture with the three colour-coded regions of interest identified. (b) The mitochondrial Ca^{2+} concentration changes, in response to the local basal (green area) Ca^{2+} uncaging, in the three regions (colour coded as in the transmitted light picture). It can be seen that only the mitochondria near the basal plasma membrane react initially, but later there are rather small increases also in the perigranular region.

accumulation in the mitochondria. The peak of the Ca^{2+}-dependent current did, however, occur earlier than the peak of the mitochondrial Ca^{2+} concentration. Although it has been proposed that mitochondria possess a Ca^{2+}-induced Ca^{2+} release (CICR) mechanism *in vitro* (Ichas *et al*., 1997), the second uncaging of NP-EGTA consistently failed to evoke signs of CICR from the mitochondria in our intact cells. In all the 11 cells tested, the second uncaging of caged Ca^{2+} resulted in further mitochondrial Ca^{2+} uptake, rather than release (Figure 7A, c).

We also uncaged Ca^{2+} locally in the basal region, outlined in green in Figure 7B, a, and measured the mitochondrial Ca^{2+} uptake in three different areas (green, red and black). In this case the mitochondrial Ca^{2+} uptake was localized to the basal area (green) in which the uncaging had occurred. In the two other areas there were initially no signs of mitochondrial Ca^{2+} uptake, although subsequent Ca^{2+} uncagings induced small rises in $[Ca^{2+}]_m$ in the perigranular region (red) (Figure 7B, b) (n = 6).

Next, we loaded Rhod-2-AM and NP-EGTA-AM into the same cell and uncaged Ca^{2+} in a very small area within the nucleus. As shown in Figure 8A, a and b, after repetitive Ca^{2+} uncaging in a small area within the nucleus (red dotted circle), the perinuclear mitochondria (blue area) were the first to take up Ca^{2+}. Later, mitochondria in the lateral area of the cell (green circle) took up Ca^{2+}.

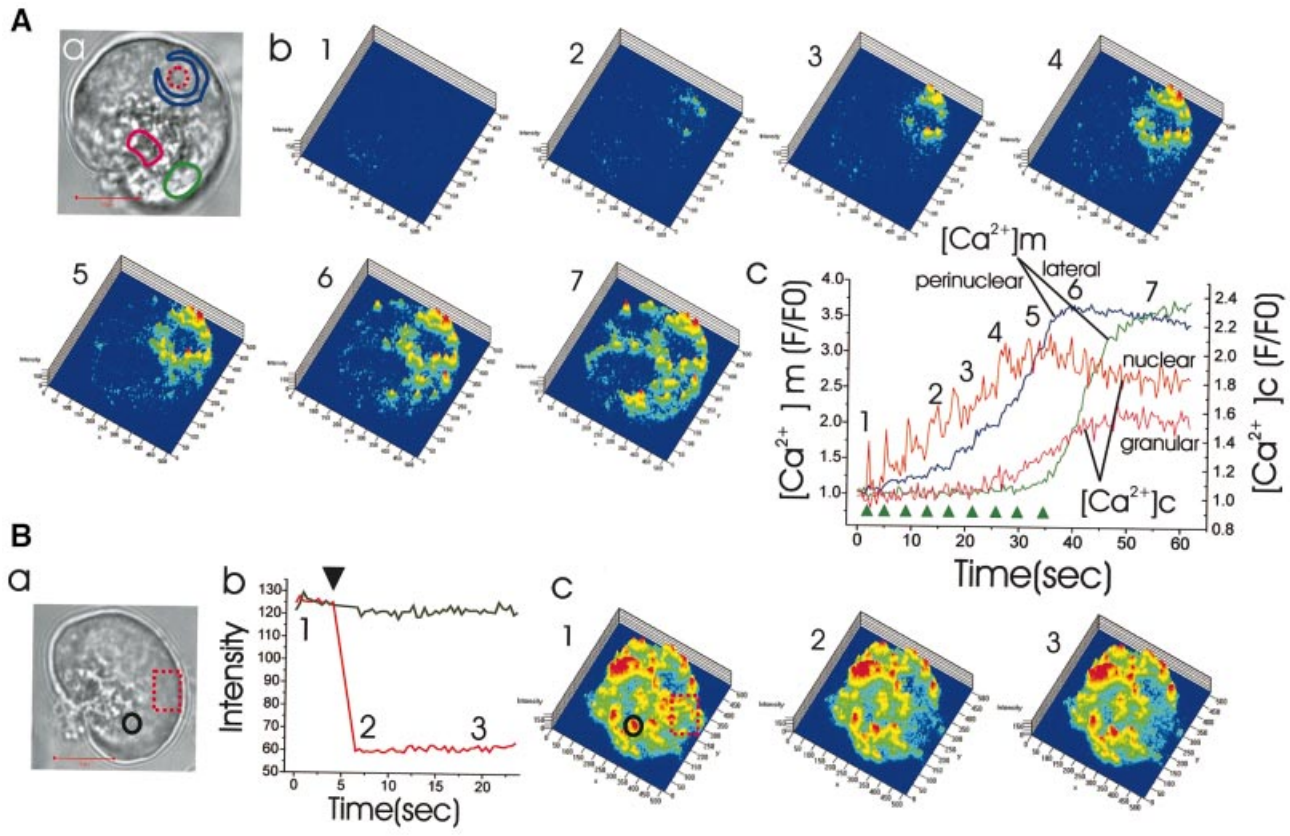

Fig. 8. Local Ca^{2+} uncaging in the nucleus results in specific Ca^{2+} uptake into the mitochondria located just around the nucleus and local bleaching experiment indicates that different mitochondrial groups may not communicate directly. (**A**) Repetitive nuclear Ca^{2+} uncagings result in increasing Ca^{2+} uptake exclusively into the perinuclear mitochondrial ring, until suddenly towards the end of the experiment, all mitochondria take up Ca^{2+}. (a) The transmitted light picture shows the site of Ca^{2+} uncaging (red broken circle) and the colour-coded regions of interest. Length of red bar corresponds to 10 μm. (b) Series of Rhod-2 fluorescence images showing increasing Ca^{2+} concentration in the perinuclear mitochondrial ring (images 1–5). The last couple of uncagings result in a generalized increase in the cytosolic Ca^{2+} concentration, which causes major Ca^{2+} uptake into the mitochondria, also in other regions (images 6 and 7). (c) Graphs representing the time courses of the Ca^{2+} concentration changes in the cytosol and the mitochondria in different regions following the repetitive Ca^{2+} uncagings in the nucleus (arrowheads). (**B**) An area of a cell represented by the broken red rectangle in (a) was bleached and the changes in the Rhod-2 fluorescence intensity, which had just been increased by uncaging of caged Ca^{2+}, were monitored. Length of red bar represents 10 μm. (b) Graph showing that there is a dramatic decrease in the fluorescence intensity in the bleached area (red), which is not transmitted to the neighbouring region (black). (c) Fluorescence images obtained at the times indicated in (b).

Figure 8A, c shows simultaneous measurements of the Ca^{2+} concentration changes in the nucleoplasm and the cytosol in the granular area as well as in the mitochondria in the perinuclear and lateral regions. The $[Ca^{2+}]_m$ rise in the lateral region was considerably delayed as compared with the $[Ca^{2+}]_m$ rise in the perinuclear area, demonstrating the buffering power of the perinuclear mitochondria. Similar results were obtained from six cells. These data explain why the nucleus is not easily affected by short-lasting cytosolic Ca^{2+} changes (Gerasimenko *et al*, 1996; Cancela *et al*., 2000), whereas the steady-state Ca^{2+} concentration in the nucleoplasm reflects the cytosolic Ca^{2+} concentration reasonably well (Brini *et al*., 1993; Mogami *et al*., 1998).

Dye bleaching experiments

The results presented so far show that mitochondria in distinct regions can react to local changes in the cytosolic Ca^{2+} concentration without necessarily influencing $[Ca^{2+}]_m$ in other regions. We therefore tested the possible luminal connection between mitochondria in different areas. Figure 8B, a shows the transmitted light picture of a cell under investigation. We observed a marked rise in $[Ca^{2+}]_m$ in all the regions after global cytosolic Ca^{2+} uncaging. Thereafter, we bleached rapidly one area of the cell (red dotted rectangle in Figure 8B, a and c) using the maximum power of our UV laser (351, 364 nm line). This resulted in complete bleaching of mitochondrial fluorescence in this part of the cell. There was no restoration of fluorescence intensity and the fluorescence intensities in the neighbouring peripheral basal as well as perigranular mitochondria were not changed at all (Figure 8B, b and c, similar data obtained in seven cells). Although the possibility cannot be excluded that UV laser-induced damage could in some manner isolate otherwise communicating organelles, the simplest interpretation of our data indicates that in normal pancreatic acinar cells the mitochondria are not luminally connected.

Mitochondrial Ca^{2+} uptake specifically due to Ca^{2+} entry from external solution

The result shown in Figure 7B, demonstrating that local Ca^{2+} uncaging in the basal area causes selective Ca^{2+} uptake in mitochondria in that region, might indicate that

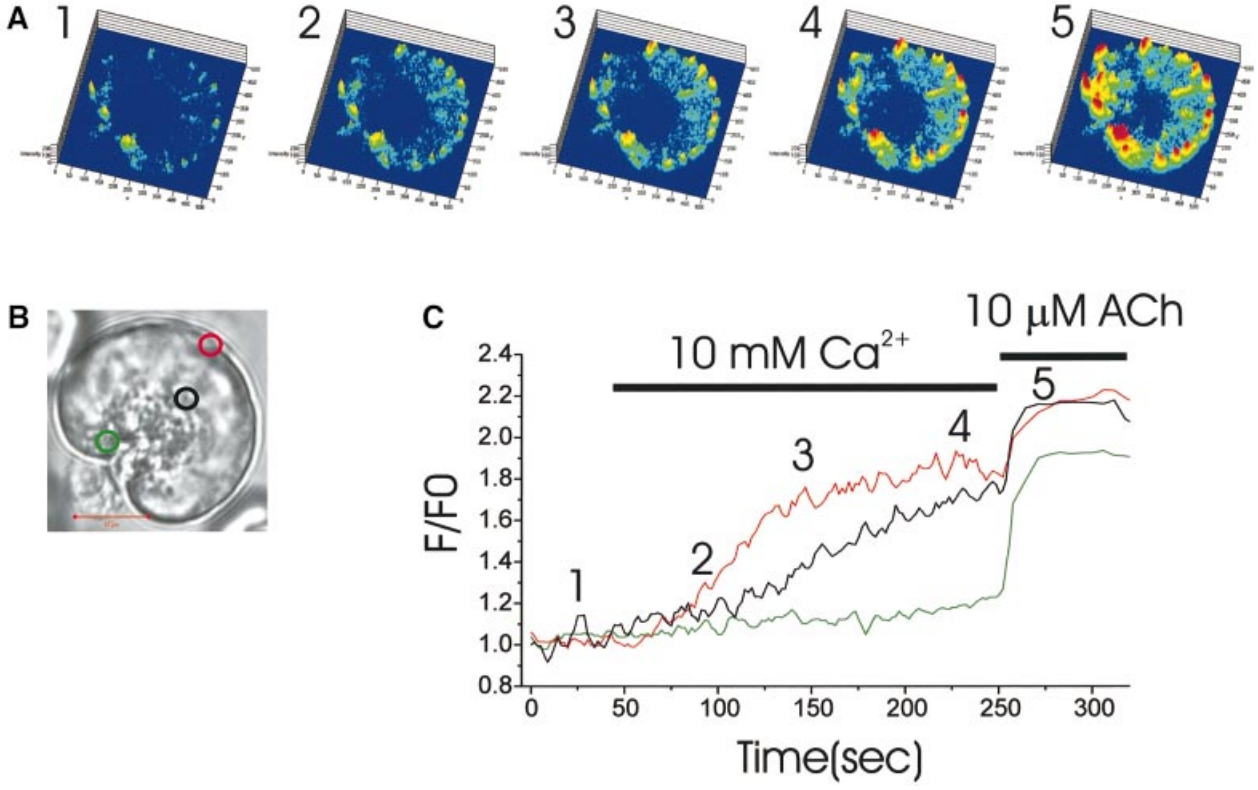

Fig. 9. Basolateral mitochondrial Ca^{2+} uptake due to store-operated Ca^{2+} entry. In this series of experiments, cells were exposed to a Ca^{2+}-free solution containing 0.5 μM thapsigargin for 3 min to partially deplete internal Ca^{2+} stores. A high external Ca^{2+} concentration (10 mM) was then introduced, allowing Ca^{2+} entry through store-operated Ca^{2+} channels. (**A**) Series of Rhod-2 fluorescence images showing increasing Ca^{2+} accumulation in the peripheral mitochondria during the period of Ca^{2+} entry (images 1–4) and finally the increase in the Ca^{2+} concentration in the apically located mitochondria after ACh stimulation (image 5). The numbers correspond in time to those shown in (C). (**B**) Transmitted light image of the cell under investigation with the three colour-coded regions identified. Length of red bar corresponds to 10 μm. (**C**) The three coloured traces represent mitochondrial Ca^{2+} measurements (Rhod-2) in the three correspondingly colour-coded regions identified in (B). It is seen that by far the most marked rise in the mitochondrial Ca^{2+} concentration occurred in the region very close to the basal membrane. At the end of the experiment, a high dose of ACh is applied, causing further increase in the mitochondrial Ca^{2+} concentration, but this time most marked in the area very close to the apical membrane [see also image 5 in (A)].

Ca^{2+} entry across the basal membrane could selectively affect the peripheral basolaterally located mitochondria. Ca^{2+} entry through the basal membrane can refill the intracellular ER Ca^{2+} store after agonist-induced depletion (Mogami *et al*., 1997) and it has been shown recently that respiring mitochondria determine the pattern of activation and inactivation of the store-operated Ca^{2+} current (Gilabert and Parekh, 2000). We therefore investigated directly whether mitochondria in the peripheral basolateral area, which is very close to the plasma membrane, could preferentially respond to store-operated Ca^{2+} influx. Ca^{2+} was liberated from the ER store by exposing the cells to a Ca^{2+}-free external solution containing a high concentration (0.5 μM) of the ER Ca^{2+} pump inhibitor thapsigargin for a relatively short period (3 min). This results in a substantial reduction in the ER Ca^{2+} concentration (Mogami *et al*., 1998). When the external Ca^{2+}-free solution is then replaced by a solution containing a high Ca^{2+} concentration (10 mM), Ca^{2+} entry should occur through store-operated channels (Parekh and Penner, 1997). The result of such an experiment is illustrated in Figure 9. Admission of the external solution with the high Ca^{2+} concentration resulted initially in a selective rise in $[Ca^{2+}]_m$ in the basolateral region of the cell very close to the plasma membrane (Figure 9). Later, there was also a more modest rise in $[Ca^{2+}]_m$ in the perigranular region. At the end of the experiment, a supramaximal concentration of ACh was applied. This resulted in a rise in $[Ca^{2+}]_m$ that was most marked near the apical (luminal) membrane. The relatively minor effect of ACh stimulation indicates that refilling of the ER store had not occurred during the period of Ca^{2+} entry, since the effect of thapsigargin is irreversible. On the other hand, the fact that ACh did induce a rise in $[Ca^{2+}]_m$ near the apical membrane (green circle, green curve, image 5) indicates that the relatively short period of thapsigargin exposure had not completely depleted the ER store of Ca^{2+}. Complete depletion of the ER store takes 10–15 min. We performed five separate experiments of the type shown in Figure 9, all with similar results.

Discussion

Figure 10 summarizes our findings. In addition to the perigranular mitochondria described previously (Tinel *et al*., 1999; Straub *et al*., 2000), we have identified two separate groups of mitochondria located in the peripheral basolateral area close to the plasma membrane and in the perinuclar area. We have now shown that each of these

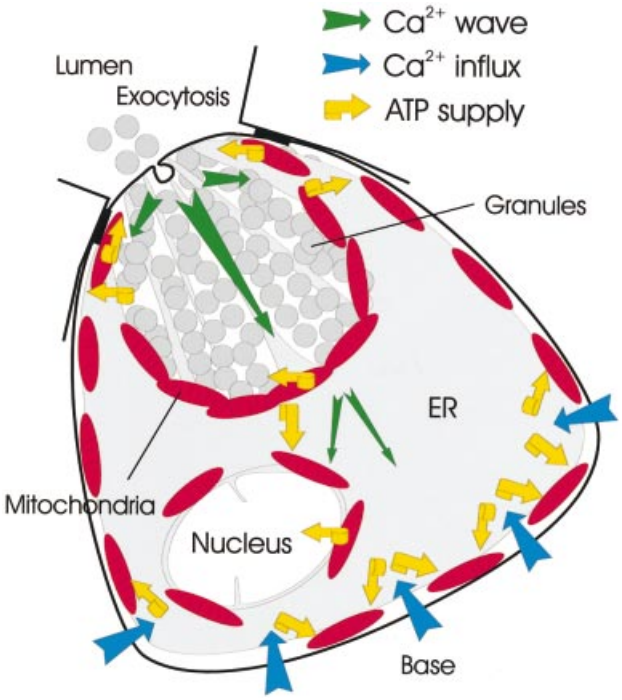

Fig. 10. Schematic drawing illustrating the locations of the different mitochondrial groups together with directions of Ca^{2+} transport and indications of ATP supply. For further details see text.

three groups of mitochondria responds specifically to cytosolic Ca^{2+} signals in their immediate environment. It is not entirely clear to what extent electrical and chemical coupling between mitochondria occurs in different cell types. A recent study of COS-7 cells indicates that as far as electrical coupling is concerned, the situation may be dynamic, with mitochondrial units spontaneously connecting and disconnecting (De Giorgi *et al*., 2000). Our local bleaching experiments (Figure 8) indicate that the Ca^{2+}-sensitive dye Rhod-2 may not move between mitochondrial areas. At least in normal pancreatic acinar cells, the mitochondria in different regions are apparently not sufficiently luminally connected to allow passage of small molecules along chemical gradients. It is therefore convenient to discuss the function of each of the three mitochondrial groups separately.

The perigranular mitochondria

The perigranular mitochondrial belt was described by Tinel *et al*. (1999), but here we have for the first time shown directly that cytosolic Ca^{2+} spiking leads to Ca^{2+} uptake into these mitochondria (Figure 5), thereby directly demonstrating their ability to perform a barrier function. We have now also identified a specific subgroup of perigranular mitochondria situated very close to the apical plasma membrane. These mitochondria are close to the primary Ca^{2+} release sites in the granular area (trigger zone) (Kasai *et al*., 1993; Thorn *et al*., 1993; Mogami *et al*., 1997; Cancela *et al*., 2000) and are particularly sensitive to the early stages of agonist-induced Ca^{2+} release (Figure 2). This is consistent with data showing that even in the case of supramaximal stimulation, when the $[Ca^{2+}]_i$ signal spreads rapidly all over the cell, the $[Ca^{2+}]_i$ rise is largest in the apical region (Ito *et al*., 1997).

Under physiological stimulation, the amounts of Ca^{2+} released from the ER during each spike are so small that the fall in $[Ca^{2+}]_{ER}$ is normally undetectable (Park *et al*., 2000). Nevertheless, our new results show that these short-lasting cytosolic Ca^{2+} spikes, which are largely confined to the granular region, cause clearly measurable Ca^{2+} uptake in the mitochondria located most apically in the perigranular belt (Figure 5). This indicates close contacts between the Ca^{2+} release sites in the ER and the apical mitochondria, as already described in other systems (Rizzuto *et al*., 1998). During each local $[Ca^{2+}]_i$ spike in the granular region, there is an exocytotic response (capacitance increase) (Maruyama and Petersen, 1994). The apical mitochondria are therefore likely to be most important for stimulus–metabolism coupling under physiological conditions. This makes sense, since exocytotic secretion, which requires a high ATP concentration (Baker and Knight, 1978), is exclusively taking place across the apical membrane (Palade, 1975).

The peripheral mitochondria near the basal plasma membrane

We have demonstrated that store-operated Ca^{2+} entry, which is important for refilling empty ER stores with Ca^{2+} (Parekh and Penner, 1997), is sensed by the peripheral basolateral mitochondria. This is in agreement with the recent demonstration (Gilabert and Parekh, 2000) that respiring mitochondria play a role both in the activation and inactivation phases of the store-operated Ca^{2+} entry. This requires Ca^{2+} uptake into mitochondria placed very close to the Ca^{2+} entry channels (Figure 9). This process would increase ATP production, which would be helpful locally, as Ca^{2+} entering the cell is taken up into the ER by powerful Ca^{2+}-activated ATPases (Mogami *et al*., 1997). Ca^{2+} uptake into both the ER and the mitochondria would tend to reduce $[Ca^{2+}]_i$ near the Ca^{2+} entry sites and therefore help diminish the strong negative feedback effect of Ca^{2+} on the open state probability of the store-operated Ca^{2+} channels (Parekh and Penner, 1997), which would otherwise effectively stop entry.

The perinuclear mitochondria

To what extent the Ca^{2+} concentrations in the nucleoplasm and the cytosol can be regulated independently is still controversial (Rogue and Malviya, 1999). The nuclear pore complexes are normally permeable to Ca^{2+} (Brini *et al*., 1993; Gerasimenko *et al*., 1995; Lipp *et al*., 1997) but, at least temporarily, discrepancies between the Ca^{2+} levels inside and outside the nuclear envelope can occur (Rogue and Malviya, 1999). Intermediate doses of ACh can initiate cytosolic Ca^{2+} signals in the granular area that spread to the basal part of the cell, except the nucleus (Gerasimenko *et al*., 1996). The perinuclear ring of mitochondria (Figure 1C), which takes up Ca^{2+} specifically when Ca^{2+} is uncaged in the nucleus (Figure 8A), could play a role in protecting the nucleus against invasion of $[Ca^{2+}]_i$ signals. The nucleus has potential for generating its own Ca^{2+} signals (Gerasimenko *et al*., 1995; Malviya and Rogue, 1998). The perinuclear mitochondrial barrier could play a role by helping to confine such signals, initiated by release through the inner nuclear membrane, to the nucleoplasm and at the same time supply ATP locally. Ca^{2+} signals in the perinuclear mitochondria could also be

important for the regulation of the energetics of nuclear transport and possibly play a role in triggering release of activators of apoptosis from perinuclear mitochondria.

Conclusion

The spatio-temporal pattern of $[Ca^{2+}]_i$ signals depends on agonist type and concentration (Petersen *et al*., 1991) and this is important for understanding differential physiological and pathophysiological regulation (Petersen *et al*., 1994; Parekh, 2000). Our new results show that different groups of functionally unconnected regional mitochondria can sense $[Ca^{2+}]_i$ signals in their immediate environment (Figure 10). The most restricted $[Ca^{2+}]_i$ signals in space and time are the repetitive short-lasting Ca^{2+} spikes that are confined to the granular region (Thorn *et al*., 1993), because of the perigranular mitochondrial Ca^{2+} buffer barrier (Figures 5 and 10). These spikes control exocytotic secretion (Maruyama and Petersen, 1994) through the apical membrane (Palade, 1975), and the local ATP supply from the apical part of the perigranular ring is therefore most likely to be of major physiological significance. Ca^{2+} for stimulus–secretion coupling is ultimately derived from the external solution and enters the acinar cell across the basal membrane. We have shown previously (Mogami *et al*., 1997; Park *et al*., 2000) that Ca^{2+} is transported across the cell, shielded from the cytosol, by an operational ER tunnel. Ca^{2+} is therefore always available for release from the ER extensions in the granular area. Ca^{2+} entry into the basal part of the ER tunnel depends on thapsigargin-sensitive Ca^{2+} pumps in the ER (Mogami *et al*., 1997). The peripheral mitochondria, which take up Ca^{2+} specifically during store-operated Ca^{2+} entry (Figures 9 and 10), must therefore play an important role in supplying the ER Ca^{2+} uptake machinery with the necessary ATP. Finally, the nucleus may have special problems in relation to Ca^{2+} signalling. During normal secretory events, it is not desirable to involve the nucleus. Indeed, we have shown previously that when the Ca^{2+} signal escapes from the granular region, the nuclear area is still somewhat protected against invasion by Ca^{2+} waves (Gerasimenko *et al*., 1996). The perinuclear mitochondrial ring (Figures 8 and 10) is likely to play an important role in this protection. The perinuclear mitochondria could also play an important role in confining signals generated inside the nucleus to this organelle.

Materials and methods

Cell preparation

Fresh mouse pancreatic acinar cells were isolated after collagenase treatment, as previously described (Osipchuk *et al*., 1990) and used within 2 h. All experiments were performed at room temperature (22–24°C). Mag-fluo-4-AM, fluo-4-AM, MitoTracker Green FM, Hoechst 33342, Rhod-2-AM and NP-EGTA-AM were purchased from Molecular Probes, and the other chemicals were from Sigma Co.

Solutions

The extracellular bathing solution contained (in mM): NaCl 140, KCl 4.7, $MgCl_2$ 1.13, $CaCl_2$ 1, glucose 10 and HEPES 10. pH was adjusted to 7.3 by NaOH. We used two different intracellular pipette solutions. One contained (in mM): KCl 135, $MgCl_2$ 1.13, NaCl 20, HEPES 10, Na_2ATP 2, EGTA 0.1; pH was 7.2, adjusted by KOH. In the other solution we replaced 0.1 mM EGTA with 10 mM BAPTA + 2 mM Ca^{2+}.

Dye-loading procedures

For visualization of mitochondria, isolated cells were incubated with 10 μM MitoTracker Green FM for 30 min at 37°C. For visualization of nuclei, Hoechst 33342 was added to the bathing solution on the microscope stage to a concentration of ~100 μg/ml. To stain the ER, we incubated cells in a solution containing 0.3–1 μM ERtracker (Molecular Probes) for 15–30 min at 37°C. For imaging of Ca^{2+} in intracellular stores, cells were incubated with 4–6 μM Mag-fluo-4-AM and 0.01% pluronic acid for 20–30 min. For mitochondrial Ca^{2+} measurements, cells were incubated with Rhod-2-AM and 0.01% pluronic acid for 20–30 min at 37°C. For combined mitochondrial and cytosolic Ca^{2+} measurements, the cells were washed after loading of Rhod-2 and then incubated with 2.5 μM fluo-4-AM for 20 min at 22°C, For experiments with uncaging of caged Ca^{2+}, NP-EGTA was loaded into the cells by incubation in a solution containing 10 μM NP-EGTA-AM for 30 min. To remove cytosolic indicators, we used the patch–clamp whole-cell configuration (Mogami *et al*., 1998). The same pipette was used to introduce calcium buffer into the cell. The patch pipette contained 0.1 mM EGTA or a 10 mM BAPTA/2 mM Ca^{2+} mixture. Some experiments with Mag-fluo-4 and/or Rhod-2 were performed on intact cells, without unloading the cytosolic calcium indicator.

Confocal imaging, photobleaching and uncaging

Confocal imaging was performed using a Zeiss LSM510 confocal system. This system allows rapidly alternating excitation of multiple fluorophores, thus reducing cross-talk. Also, accurate spatially restricted exposure of laser light can be achieved and this was used for the uncaging and bleaching experiments. Rhod-2 was excited with a 543 nm laser line and emission collected through a BP560-615 or LP560 filter. Fluo-4, Mag-fluo-4 and MitoTracker Green-FM were excited using 488 nm laser light. Emitted light was collected using a BP505-550 or LP505 filter. Hoechst 33342 was excited with UV laser light (351 nm/364 nm) and emission collected through a BP385-470 filter. We used near-maximal power of UV laser lines (351 nm/364 nm) to induce fast bleaching of Rhod-2 and adequate lower power for uncaging of NP-EGTA. Bleaching/uncaging were combined with simultaneous confocal imaging. For the image analysis, we used Zeiss confocal 510 image software as well as software developed by ourselves.

Electrophysiology

Standard patch–clamp whole-cell current recording (Hamill *et al*., 1981) was used. The electrophysiological recording of Ca^{2+}-dependent current (Petersen, 1992) was made using the EPC-8 amplifier and Pulse software (HEKA). The pipette resistance was 2–3 MΩ. The detailed procedure has been described previously (Thorn and Petersen, 1992).

Acknowledgements

We thank Nina Burdakova and Mark Houghton for technical assistance. This work was supported by a Medical Research Council (MRC) Programme Grant. M.C.A. is a Wellcome Trust Prize PhD student. O.H.P. is an MRC Research Professor.

References

Baker,P.F. and Knight,D.E. (1978) Calcium-dependent exocytosis in bovine adrenal medullary cells with leaky plasma membranes. *Nature*, **276**, 620–622.

Brini,M., Murgia,M., Pasti,L., Picard,D., Pozzan,T. and Rizzuto,R. (1993) Nuclear Ca^{2+} concentration measured with specifically targeted recombinant aequorin. *EMBO J.*, **12**, 4813–4819.

Cancela,J.M., Gerasimenko,O.V., Gerasimenko,J.V., Tepikin,A.V. and Petersen,O.H. (2000) Two different but converging messenger pathways to intracellular Ca^{2+} release: the roles of nicotinic acid adenine dinucleotide phosphate, cyclic ADP-ribose and inositol trisphosphate. *EMBO J.*, **19**, 2549–2557.

De Giorgi,F., Lartigue,L. and Ichas,F. (2000) Electrical coupling and plasticity of the mitochondrial network. *Cell Calcium*, **28**, 365–370.

Denton,R.M. and McCormack,J.G. (1990) Ca^{2+} as a second messenger within mitochondria of the heart and other tissues. *Annu. Rev. Physiol.*, **52**, 451–466.

Duchen,M.R. (2000) Mitochondria and Ca^{2+} in cell physiology and pathophysiology. *Cell Calcium*, **28**, 339–348.

Gerasimenko,O.V., Gerasimenko,J.V., Tepikin,A.V. and Petersen,O.H. (1995) ATP-dependent accumulation and inositol trisphosphate- or

cyclic ADP-ribose-mediated release of Ca^{2+} from the nuclear envelope. *Cell*, **80**, 439–444.

Gerasimenko,O.V., Gerasimenko,J.V., Petersen,O.H. and Tepikin,A.V. (1996) Short pulses of acetylcholine stimulation induce cytosolic Ca^{2+} signals that are excluded from the nuclear region in pancreatic acinar cells. *Pflugers Arch.*, **432**, 1055–1061.

Gilabert,J.A. and Parekh,A.B. (2000) Respiring mitochondria determine the pattern of activation and inactivation of the store-operated Ca^{2+} current I_{CRAC}. *EMBO J.*, **19**, 6401–6407.

Gonzalez,A., Schulz,I. and Schmid,A. (2000) Agonist-evoked mitochondrial Ca^{2+} signals in mouse pancreatic acinar cells. *J. Biol. Chem.*, **275**, 38680–38686.

Hajnoczky,G., Robb-Gaspers,L.D., Seitz,M.B. and Thomas,A.P. (1995) Decoding of cytosolic calcium oscillations in the mitochondria. *Cell*, **82**, 415–424.

Hamill,O.P., Marty,A., Neher,E., Sakmann,B. and Sigworth,F.J. (1981) Improved patch-clamp techniques for high-resolution current recording from cells and cell-free membrane patches. *Pflugers Arch.*, **391**, 85–100.

Ichas,F., Jouaville,L.S. and Mazat,J.P. (1997) Mitochondria are excitable organelles capable of generating and conveying electrical and calcium signals. *Cell*, **89**, 1145–1153.

Ito,K., Miyashita,Y. and Kasai,H. (1997) Micromolar and submicromolar Ca^{2+} spikes regulating distinct cellular functions in pancreatic acinar cells. *EMBO J.*, **16**, 242–251.

Jouaville,L.S., Pinton,P., Bastianutto,C., Rutter,G.A. and Rizzuto,R. (1999) Regulation of mitochondrial ATP synthesis by calcium: Evidence for a long-term metabolic priming. *Proc. Natl Acad. Sci. USA*, **96**, 13807–13812.

Kasai,H., Li,Y.X. and Miyashita,Y. (1993) Subcellular distribution of Ca^{2+} release channels underlying Ca^{2+} waves and oscillations in exocrine pancreas. *Cell*, **74**, 669–677.

Lawrie,A.M., Rizzuto,R., Pozzan,T. and Simpson,A.W.M. (1996) A role for calcium influx in the regulation of mitochondrial calcium in endothelial cells. *J. Biol. Chem.*, **271**, 10753–10759.

Lipp,P., Thomas,D., Berridge,M.J. and Bootman,M.D. (1997) Nuclear calcium signalling by individual cytoplasmic calcium puffs. *EMBO J.*, **16**, 7166–7173.

Malviya,A.N. and Rogue,P.J. (1998) 'Tell me where is calcium bred': clarifying the roles of nuclear calcium. *Cell*, **92**, 17–23.

Maruyama,Y. and Petersen,O.H. (1994) Delay in granular fusion evoked by repetitive cytosolic Ca^{2+} spikes in mouse pancreatic acinar cells. *Cell Calcium*, **16**, 419–430.

McCormack,J.G., Halestrap,A.P. and Denton,R.M. (1990) Role of calcium-ions in regulation of mammalian intramitochondrial metabolism. *Physiol. Rev.*, **70**, 391–425.

Mogami,H., Nakano,K., Tepikin,A.V. and Petersen,O.H. (1997) Ca^{2+} flow via tunnels in polarized cells: recharging of apical Ca^{2+} stores by focal Ca^{2+} entry through basal membrane patch. *Cell*, **88**, 49–55.

Mogami,H., Tepikin,A.V. and Petersen,O.H. (1998) Termination of cytosolic Ca^{2+} signals: Ca^{2+} reuptake into intracellular stores is regulated by the free Ca^{2+} concentration in the store lumen. *EMBO J.*, **17**, 435–442.

Montero,M., Alonso,M.T., Carnicero,E., Cuchillo-Ibanez,I., Albillos,A., Garcia,A.G., Garcia-Sancho,J. and Alvarez,J. (2000) Chromaffin-cell stimulation triggers fast millimolar mitochondrial Ca^{2+} transients that modulate secretion. *Nature Cell Biol.*, **2**, 57–61.

Osipchuk,Y.V., Wakui,M., Yule,D.I., Gallacher,D.V. and Petersen,O.H. (1990) Cytoplasmic Ca^{2+} oscillations evoked by receptor stimulation, G-protein activation, internal application of inositol trisphosphate or Ca^{2+}: simultaneous microfluorimetry and Ca^{2+}-dependent Cl^- current recording. *EMBO J.*, **9**, 697–704.

Palade,G.E. (1975) Intracellular aspects of the process of protein secretion. *Science*, **189**, 347–358.

Parekh,A. (2000) Calcium signaling and acute pancreatitis: specific response to a promiscuous messenger. *Proc. Natl Acad. Sci. USA*, **97**, 12933–12934.

Parekh,A. and Penner,R. (1997) Store depletion and calcium influx. *Physiol. Rev.*, **77**, 901–930.

Park,M.K., Petersen,O.H. and Tepikin,A.V. (2000) The endoplasmic reticulum as one continuous Ca^{2+} pool: visualization of rapid Ca^{2+} movements and equilibration. *EMBO J.*, **19**, 5729–5739.

Petersen,C.C.H., Toescu,E.C. and Petersen,O.H. (1991) Different patterns of receptor-activated cytoplasmic Ca^{2+} oscillations in single pancreatic acinar cells: dependence on receptor type, agonist concentration and intracellular Ca^{2+} buffering. *EMBO J.*, **10**, 527–533.

Petersen,O.H. (1992) Stimulus–secretion coupling: cytoplasmic calcium signals and the control of ion channels in exocrine acinar cells. *J. Physiol.*, **448**, 1–51.

Petersen,O.H., Petersen,C.C.H. and Kasai,H. (1994) Calcium and hormone action. *Annu. Rev. Physiol.*, **56**, 297–319.

Petersen,O.H., Tepikin,A.V. and Park,M.K. (2001) The endoplasmic reticulum: one continuous or several separate Ca^{2+} stores. *Trends Neurosci.*, **24**, 271–276.

Pinton,P., Drummond,R., Magalhaes,P., Brini,M., Chiesa,A., Pozzan,T. and Rizzuto,R. (2001) Ca^{2+} measurements in mitochondria. In Petersen,O.H. (ed.), *Measuring Calcium and Calmodulin Inside and Outside Cells*. Springer Laboratory Manual, Heidelberg, Germany, pp. 185–210.

Pozzan,T., Rizzuto,R., Volpe,P. and Meldolesi,J. (1994) Molecular and cellular physiology of intracellular Ca^{2+} stores. *Physiol. Rev.*, **74**, 595–636.

Pozzan,T., Magalhaes,P. and Rizzuto,R. (2000) The comeback of mitochondria to calcium signalling. *Cell Calcium*, **28**, 279–283.

Raraty,M., Ward,J., Erdemli,G., Vaillant,C., Neoptolemos,J.P., Sutton,R. and Petersen,O.H. (2000) Calcium-dependent enzyme activation and vacuole formation in the apical granular region of pancreatic acinar cells. *Proc. Natl Acad. Sci. USA*, **97**, 13126–13131.

Rizzuto,R., Pinton,P., Carrington,W., Fay,F.S., Fogarty,K.E., Lifshitz, L.S., Tuft,R.A. and Pozzan,T. (1998) Close contacts with the endoplasmic reticulum as determinants of mitochondrial Ca^{2+} responses. *Science*, **280**, 1763–1766.

Rizzuto,R., Bernadi,P. and Pozzan,T. (2000) Mitochondria as all-round players of the calcium game. *J. Physiol.*, **529**, 37–47.

Rogue,P.J. and Malviya,A.N. (1999) Calcium signals in the cell nucleus. *EMBO J.*, **18**, 5147–5152.

Rutter,G.A. and Rizzuto,R. (2000) Regulation of mitochondrial metabolism by ER Ca^{2+} release: an intimate connection. *Trends Biochem. Sci.*, **25**, 215–221.

Straub,S.V., Giovannucci,D.R. and Yule,D.I. (2000) Calcium wave propagation in pancreatic acinar cells. Functional interaction of inositol 1,4,5-trisphosphate receptors, ryanodine receptors and mitochondria. *J. Gen. Physiol.*, **116**, 547–559.

Thorn,P. and Petersen,O.H. (1992) Activation of nonselective cation channels by physiological cholecystokinin concentrations in mouse pancreatic acinar cells. *J. Gen. Physiol.*, **100**, 11–25.

Thorn,P., Lawrie,A.M., Smith,P.M., Gallacher,D.V. and Petersen,O.H. (1993) Local and global cytosolic Ca^{2+} oscillations in exocrine cells evoked by agonists and inositol trisphosphate. *Cell*, **74**, 661–668.

Tinel,H., Cancela,J.M., Mogami,H., Gerasimenko,J.V., Gerasimenko, O.V., Tepikin,A.V. and Petersen,O.H. (1999) Active mitochondria surrounding the pancreatic acinar granule region prevent spreading of inositol trisphosphate-evoked local cytosolic Ca^{2+} signals. *EMBO J.*, **18**, 4999–5008.

Received January 23, 2001; revised and accepted February 28, 2001